STAG: Smart Tools and Applications in Graphics (2020)
S. Biasotti, R. Pintus and S. Berretti (Editors)

Multisided B-spline Patches Over Extraordinary Regions

G. J. Hettinga[1] and J. Kosinka[1]

[1]Bernoulli Institute, University of Groningen, The Netherlands

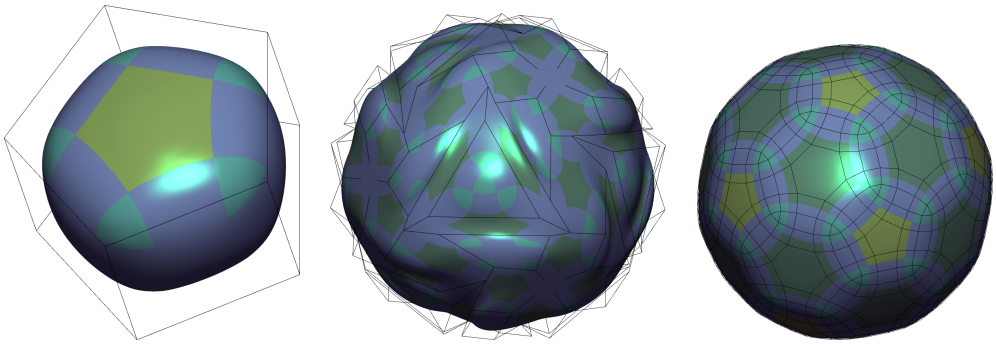

Figure 1: Three objects containing several extraordinary regions rendered using (from left to right): quadratic, cubic and quartic multisided B-spline patches. The input control meshes are shown as well.

Abstract

We propose a generalised B-spline construction that extends uniform bi-degree B-splines to multisided regions spanned over extraordinary regions in quad-dominant meshes. We show how the structure of the existing cubic multisided B-spline patch can be generalised to work with B-spline basis functions of arbitrary degree and can be spanned over extraordinary vertices as well as extraordinary faces of quad-dominant meshes. The resulting multisided surfaces are C^{d-1} continuous internally and connect with G^{d-1} continuity to adjacent regular and other multisided B-splines patches. In addition, we design several specialised functions that increase the visual quality of the patches, in both the extraordinary vertex and face settings.

CCS Concepts

•***Computing methodologies*** → ***Parametric curve and surface models;***

1. Introduction

Extraordinary regions introduce problems in the definition of B-spline surfaces and have therefore posed a long-standing challenge in computer graphics and geometric design. These extraordinary regions in quad-dominant meshes, consisting of extraordinary faces (with other than four sides) and extraordinary vertices (vertices with valency other than four), create problems in the definition of the B-spline-like basis functions. Nevertheless, many solutions exist to create smooth surfaces for these special regions, most of which focus on quad-dominant meshes.

One such solution is the use of subdivision surfaces, which generalise the subdivision rules of B-splines to arbitrary topology meshes, to be able to create surfaces over extraordinary regions. However, subdivision surfaces entail an iterative process and are typically only G^1 continuous at the limit points corresponding to extraordinary vertices/faces. While subdivision surfaces are easily evaluated in regular regions, there is no simple way to evaluate them in extraordinary regions [Sta98]. Other approaches use multiple smooth bi-degree patches surrounding extraordinary vertices [Pet02], but similar techniques do not seem to exist for extraordinary faces without involving an initial subdivision step.

The generalised multisided cubic B-spline patch [HK20] is a multisided B-spline patch that takes the structure of generalised Bézier patches [VSK16], and adapts it for use with uniform cubic B-spline basis functions. The patches introduce the notions of B-spline ribbons and extended basis functions.

As our main contribution, we further develop these multisided B-spline patches such that they generalise to:

DOI: 10.2312/stag.20201235

- arbitrary bi-degrees and
- extraordinary faces with an arbitrary number of sides,

as shown in Figure 1. We thus offer a unified treatment of both extraordinary vertices and faces in one method. The new construction is based on the generalised Bézier patch, in that it builds on many of the same elements: ribbon surfaces, generalised barycentric coordinates, and suitable blending functions.

The rest of the paper is structured as follows. In Section 2, we give an overview of related work. In Section 3 we recall both generalised barycentric coordinates and the cubic generalised B-spline patch [HK20]. In Section 4, we introduce our multisided B-spline patch construction and afterwards, in Section 5, we show several results using our patches. We discuss the proposed method and conclude the paper in Section 6.

2. Related Work

Although they solve a related problem, we mention only a few approaches, among the many that exist, that use a multitude of quadrilateral macro-elements around extraordinary vertices; the reason being that they, in contrast to our method, do not directly treat extraordinary faces. Catmull-Clark subdivision surfaces have been approximated by Gregory patches [LSNC09] to create a tangent-plane continuous surface. Loop & Schaefer use n biseptic patches [LS08] and Karčiuaskas & Peters [KP16] use bi-sextic patches to create globally G^2 surfaces. An overview of such constructions can be found in [Pet19].

There exist many types of multisided patches such as generalised Bézier patches [VSK16] and the S-patch [LD89], but it is not trivial to include these patches in B-spline surfaces. Loop & DeRose created a version of the S-patch that can be included in otherwise regular B-spline surfaces such that the S-patches join with G^1 continuity to biquadratic and bicubic regions, but the patches are of high degree and have a large number of control points. Moreover, they are well defined only over (extraordinary) faces.

The corner interpolator patches of Gregory [GLZ90] are able to interpolate arbitrary curves, derivatives and second derivatives over a multisided region. The method combines n corner surfaces into a patch that can join with G^2 continuity to neighbouring regular regions. They have been used in combination with subdivision methods to create arbitrary topology cubic B-spline surfaces [ZZZS05].

There exist other constructions based on the theory of manifolds that generalise B-splines surfaces of arbitrary degree for arbitrary topology meshes [YZ04, NG00]. A special chart is associated to each element of the mesh and the overlapping charts are combined using a partition of unity method. And while this approach influences the regular regions, which is undesirable in some applications, it leads to surfaces with arbitrary smoothness.

Multisided cubic B-spline patches [HK20], which we generalise to arbitrary degrees and further extend to extraordinary faces, are described in detail in the following section.

3. Preliminaries

Multisided patches are commonly parametrised by generalised barycentric coordiantes. We discuss these first, and then move on to cubic multisided B-spline patches.

3.1. Generalised Barycentric Coordinates

Generalised barycentric coordinates provide a coordinate system in which any point $\mathbf{p}$ on a planar polygon can be expressed as a weighted combination of the polygon's vertices. There are many types of these coordinates and an extensive overview of generalised barycentric coordinates can be found in [Flo15]. We recall the main properties of these coordinates.

With a cyclic ordering of the vertices $\mathbf{v}_i$, $i = 1,\dots,n$ of a polygon, the barycentric coordinate functions ϕ_i, $i = 1,\dots,n$ partition unity $\sum_{i=1}^{n}\phi_i = 1$, are non-negative $\phi_i \geq 0, \forall i$ on the polygon, and satisfy the barycentric property $\sum_{i=1}^{n}\phi_i(\mathbf{p})\mathbf{v}_i = \mathbf{p}$. Linear interpolation is achieved on the boundary for smooth coordinates, and at the vertices the Lagrange property is satisfied $\phi_i(\mathbf{v}_j) = \delta_{ij}$, where δ_{ij} is the Kronecker delta. For triangles the coordinates reduce to the unique barycentric coordinates. For higher valencies this uniqueness property no longer holds.

To parametrise a polygon in $\mathbb{R}^3$ we use a regular parametrisation domain, a regular polygon of valency n, which we parametrise by Wachspress coordinates [Wac75]. Although many other options exist, such as harmonic coordinates used in [SV18, VSVS20], Wachspress coordinates provide, arguably, the simplest and most efficient choice due to their closed rational form [Flo15, HBK18].

3.2. The Cubic Multisided B-spline Patch

The cubic C^2 multisided B-spline patch introduced in [HK20] is based on the generalised Bézier patch of [VSK16] and introduces the notion of B-spline ribbons. These ribbons are partial bi-degree B-spline surfaces that use special functions. The parametrisation of the ribbons is done by creating local variables per ribbon from generalised barycentric coordinates $\boldsymbol{\phi} = [\phi_1,\dots,\phi_n]$. A ribbon $\mathbf{R}_i$ has local parameters s_i and h_i that behave like bi-linear coordinates. They are constructed from the generalised barycentric coordinates corresponding to the vertices $\mathbf{v}_{i-1}$ and $\mathbf{v}_i$ of the parametrisation domain: the side parameter $s_i(\boldsymbol{\phi}) = 1-\phi_i-\phi_{i-1}$ and the distance parameter $h_i(\boldsymbol{\phi}) = \frac{\phi_i}{\phi_i+\phi_{i-1}}$. The side parameter s_i increases linearly on side Γ_i and is 0 on Γ_{i-1} and 1 on Γ_{i+1}. Similarly, the distance parameter h_i is 0 on the whole of Γ_i and increases linearly on sides Γ_{i-1} and Γ_{i+1}, and into the polygon.

The multisided patches combine n cubic B-spline ribbons. The control point layout of a cubic multisided B-spline patch is shown in Figure 2; its control points are those in the area enclosed in green. To blend everything together and to keep continuity properties of the individual ribbons, special blending functions are attached to the control points that are shared between adjacent ribbons. We can simply decompose these blending functions into left (α_i^q) and right (β_i^q) blending functions

$$\alpha_i^q = \frac{h_{i-1}^q}{h_i^d + h_{i-1}^q}, \quad \beta_i^q = \frac{h_{i+1}^q}{h_i^d + h_{i+1}^q}.$$

These blending functions are then distributed using

$$\mu^i_{jk} = \begin{cases} \alpha^3_i & j < d, \\ \alpha^3_i \beta^3_i & j = d, \\ \beta^3_i & j > d, \end{cases}$$

which then leads to the definition of a B-spline ribbon

$$\mathbf{R}_i(u,v) = \begin{cases} \sum_{j=0}^{3} \sum_{k=0}^{2} \mu^i_j \mathbf{b}^i_{jk} N^3_j(u) E^3_k(v) & u \in [0,1], \\ \sum_{j=3}^{6} \sum_{k=0}^{2} \mu^i_j \mathbf{b}^i_{jk} N^3_{j-3}(u-1) E^3_k(v) & u \in [1,2], \end{cases}$$

where $v \in [0,2]$. Here, N^3_j are the standard uniform B-spline functions and E^3_k are the extended cubic B-spline functions, defined below.

Along the direction of s_i, normal cubic B-spline basis functions are used, and along h_i, the extended basis functions E^3_j are employed. The functions are defined over the interval $[0,2]$, to be able to cover the extended domain. The first and second basis functions are simply $E^3_0(u) \equiv N^3_0(u)$, and $E^3_1(u) \equiv N^3_1(u)$ with $u \in [0,2]$. The third basis function is the piece-wise quintic function

$$E^3_2(u) = \begin{cases} N^3_2(u) & u \in [0,1], \\ \frac{2}{3}(2-u)^5 + \frac{2}{3}5(2-u)^4(u-1) & \\ +\frac{17}{30}10(2-u)^3(u-1)^2 & u \in [1,2]. \end{cases}$$

All functions $E^3_j(u) \equiv N^3_j(u)$ for $u \in [0,1]$ and the following property holds for the extended basis functions:

$$\frac{d^p E^3_j(u)}{du^p}|_{u=2} = 0,\ p = 0,1,2.$$

This last property is important, because it ensures that the ribbons $\mathbf{R}_{i+2}, \ldots, \mathbf{R}_{i-2}$ on the far side of the patch are not influenced by the basis functions of $\mathbf{R}_i$.

Finally, the ribbons can be combined into the final patch:

$$\mathbf{S}^3(\phi) = \sum_{i=0}^{n} \mathbf{R}_i(2s_i, 2h_i).$$

Similarly to the generalised Bézier patch, this patch can be made affine invariant either by normalisation by dividing it by the sum of basis and blending functions:

$$f(\phi) = \sum_{i=0}^{n} r_i(2s_i, 2d_i), \text{ where}$$
$$r_i(u,v) = \begin{cases} \sum_{j=0}^{3} \sum_{k=0}^{2} \mu^i_j N^3_j(u) E^3_k(v) & u \in [0,1], \\ \sum_{j=3}^{6} \sum_{k=0}^{2} \mu^i_j N^3_{j-3}(u-1) E^3_k(v) & u \in [1,2]. \end{cases} \quad (1)$$

Or, this sum can be used to make the patch affine invariant by attaching the deficient weight to a central control point $\mathbf{C}$, which yields

$$\mathbf{S}^3(\phi)_{\mathbf{C}} = \mathbf{C}(1 - f(\phi)) + \mathbf{S}^3(\phi).$$

In the next section, we show how we adapt the structure of this multisided cubic B-spline patch to work with uniform B-splines of any degree.

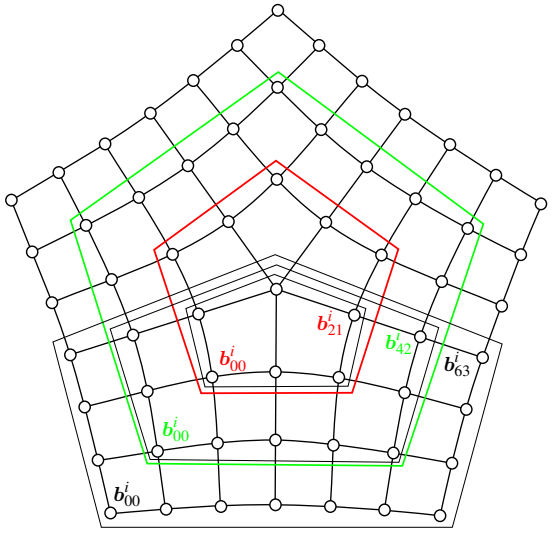

Figure 2: The control point layout for extraordinary vertex patches up to quartic patches for a pentagonal patch (valency five). The red area denotes the control points used in a quadratic patch and the green for a cubic patch, the rest of the control points are used in quartic patches. The black areas enclosed by their respective degrees denote the control points used in a single ribbon.

4. Multisided B-spline Patches

To be able to create multisided B-spline patches over extraordinary regions, the mesh has to adhere to the following conditions. For bi-degree d B-splines, the extraordinary regions have to be separated by at least $d-1$ regular vertices. However, some control meshes may not conform to this condition. Therefore, when needed, we employ degree d subdivision [Sta01], until the extraordinary regions are sufficiently separated. For even-degree (dual) subdivision schemes extraordinary vertices become extraordinary faces, and conversely for odd-degree (primal) schemes extraordinary faces turn into extraordinary vertices. The mesh with separated extraordinary regions can then be kept that way, or its dual can be computed to swap extraordinary vertices and faces again. We now detail the construction of arbitrary degree patches over both extraordinary vertices (EVs) and extraordinary faces (EFs).

4.1. Extraordinary Vertex Patches

It is possible to generate generalisations of the multisided B-spline technique to B-splines surfaces of other degree than cubic. The simplest and most straightforward generalisation, other than bilinear B-splines, is the case of biquadratic B-spline surfaces. The difference in this case is that each ribbon is just a single B-spline surface consisting of 3 columns of control points with two rows each. As with the cubic case again we need to ensure that the derivative and positional contributions of each ribbon $\mathbf{R}_i$ vanish on $\Gamma_{i+2}, \ldots, \Gamma_{i-2}$. We only need to ensure that all contributions up to the first derivative vanish as standard uniform biquadratic surfaces are only C^1 continuous. The ribbon basis functions associated with the first row of control points is $E^2_0(u) = N^2_0(u)$, which is the first of standard uni-

form quadratic B-spline functions. The second row is more complicated and, analogously to the cubic case, we need a higher degree function to ensure that all derivatives vanish. In this case a cubic function is sufficient

$$E_2^1(u) = \frac{1}{2}(1.0-u)^3 + \frac{5}{2}(1.0-u)^2 u.$$

The distribution of the blending functions α_i^2 and β_i is also analogous, in that they overlap in the middle column of control points for each ribbon. The degree of each term in the blending functions needs to be just quadratic.

Increasing the degree requires increased separation of extraordinary vertices, as discussed above. To generalise biquartic B-spline surfaces, each B-spline ribbon would need to be created out of three pieces. This would require that extraordinary vertices are at least twice removed from each another. Each quartic B-spline ribbon consists out of four rows of control points. Similarly to the cubic case we need to again create specially extended basis functions that now vanish up to the third derivative. As in the cubic case, the first three basis functions are simply the continuation of the quartic B-spline basis kernel. The last function does not exist in quartic form, and instead to be able to make all derivatives vanish and to create a C^3 join at the interval split point we need a septic function to do so.

As can be seen from the quadratic and the quartic case, this process of requiring more separate surface pieces per ribbon surface and increasing the parametric domain will continue. The same thing can be said about the separation between extraordinary vertices. Therefore we can develop a general formulation of a multisided B-spline of arbitrary degree.

The EV patch ribbons are piece-wise surfaces composed out of $d-1$ polynomial pieces. Each piece-wise surface has $d-1$ rows and d columns of control points, totalling $d \times (d+1)$ points. Then the ribbon definition is

$$\mathbf{R}_i^d(u,v) = \begin{cases} \sum_{j=0}^{d+0}\sum_{k=0}^{d-1} \mathfrak{v}_{jk}^i \mathbf{b}_{jk}^i N_{j-0}^d(u-0) E_k^d(v) & u \in [0,1], \\ \vdots & \vdots \\ \sum_{j=e}^{d+e}\sum_{k=0}^{d-1} \mathfrak{v}_{jk}^i \mathbf{b}_{jk}^i N_{j-e}^d(u-e) E_k^d(v) & u \in [d-2,d-1], \end{cases}$$

where $e = d-2$ and $v \in [0,d-1]$. The functions E_{d-1}^d restricted to the last knot-interval $[d-2,d-1]$ can be represented as Bézier polynomials of degree $2d-1$ for which the first $d-1$ coefficients c_i can be found by solving the system $\mathbf{PQx} = \mathbf{b}$, where

$$\mathbf{P} = \begin{bmatrix} 1 & & & \\ & \prod_{i=1}^{1}(2d-1-i) & & \\ & & \ddots & \\ & & & \prod_{i=1}^{d-1}(2d-1-i) \end{bmatrix},$$

$$\mathbf{Q} = \begin{bmatrix} 1 & & \\ (-1)^1\binom{1}{0} & (-1)^2\binom{1}{1} & \\ \vdots & \ddots & \\ (-1)^1\binom{d-1}{0} & \cdots & (-1)^d\binom{d-1}{d-1} \end{bmatrix}$$

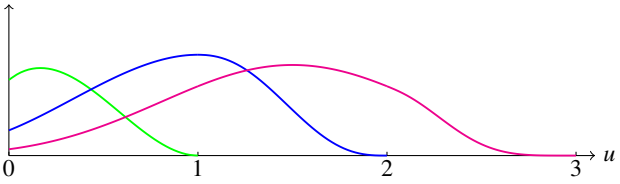

Figure 3: The quadratic (green), cubic (blue) and quartic (magenta) extended basis functions used in the construction of the multisided B-spline EV patches.

and

$$\mathbf{x} = \begin{bmatrix} c_0 \\ \vdots \\ c_{d-1} \end{bmatrix}, \quad \mathbf{b} = \begin{bmatrix} N_{d-1}^{2d-1}|_{u=d-2} \\ \vdots \\ \frac{d^{d-1}N_{d-1}^{2d-1}}{du^{d-1}}|_{u=d-2} \end{bmatrix}.$$

Again, the remaining coefficients can be set to zero so that all derivatives vanish at the end of the interval and finally the function needs to be shifted by $d-1$ intervals. In the quadratic case, the extended basis function is $E_1^2(u) = \frac{1}{2}(1-u)^3 + 5(1-u)^2 u$, and in the quartic case we get

$$E_3^4(u) = \begin{cases} N_3^4(u), & u \in [0,2], \\ \frac{11}{24}(1-v)^7 + 7\frac{65}{168}(1-v)^6 v + & \\ 21\frac{103}{336}(1-v)^5 v^2 + 35\frac{383}{1680}(1-v)^4 v^3 & u \in [2,3], \end{cases}$$

where $v = (u-2)$. Naturally, $E_j^p(u) \equiv N_k^p(u), p \in [0,d-2]$. Figure 3 shows the extended basis functions for quadratic, cubic and quartic patches.

A patch of bi-degree d needs to blend $d-1$ rows and columns of its control mesh functions, and thus the following blending function distribution is applied

$$\mathfrak{v}_{jk}^i = \begin{cases} \alpha_i^d & j < d, \\ \alpha_i^d \beta_i^d & j = d, \\ \beta_i^d & j > d. \end{cases}$$

The complete patch definition is then

$$\mathbf{S}^d(\phi) = \sum_{i=0}^{n} \mathbf{R}_i((d-1)s_i, (d-1)h_i).$$

Internally the patches are C^{d-1} continuous, and connect with G^{d-1} continuity to adjacent B-spline patches (see Section 4.3).

4.2. Extraordinary Face Patches

Patches spanned over extraordinary faces are similar to the extraordinary vertex patches. However, there are some fundamental differences. The ribbons for these patches are composed out of a greater number of pieces than for the EV patches. This has the advantage that the EF patches do not require the special extended functions $E_k^d(u)$. The B-spline ribbons consist out of d pieces and again have d rows and $2d$ columns of control points. Figure 4 shows the control net for these patches for quadratic up to quartic degrees. The

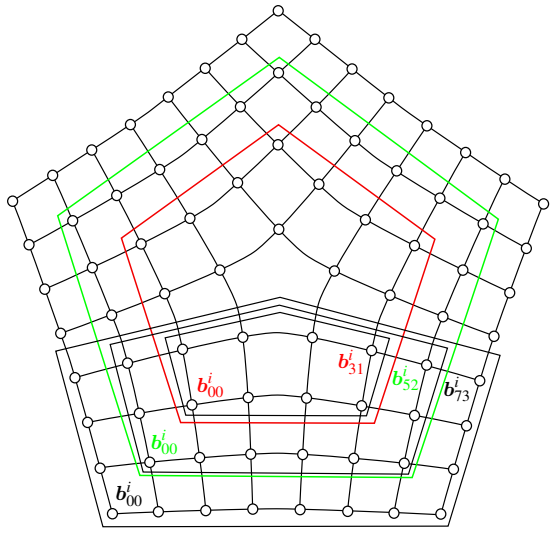

Figure 4: The control point layout for extraordinary face patches up to quartic patches for a pentagonal patch (valency 5). The red area denotes the control points used in a quadratic patch and the green for a cubic patch, the rest of the control points are used in quartic patches. The black areas enclosed by their respective degrees denote the control points used in a single ribbon.

ribbon parametrisation extends far enough into the patch to let the first $d-1$ B-spline basis functions vanish and no special extended basis functions are needed. Therefore, the ribbon definition is

$$\mathbf{R}^d_i(u,v)=\begin{cases}\sum_{j=0}^{d+0}\sum_{k=0}^{d-1}\omega^i_{jk}\mathbf{b}_{jk}N^d_{j-0}(u-0)N^d_k(v) & u\in[0,1],\\ \vdots & \vdots\\ \sum_{j=c}^{d+c}\sum_{k=0}^{d-1}\omega^i_{jk}\mathbf{b}_{jk}N^d_{j-c}(u-c)N^d_k(v) & u\in[d-1,d],\end{cases}$$

with $c=d-1$ and $v\in[0,d]$. The ribbons use the (same) blending functions

$$\omega^i_{jk}=\begin{cases}\alpha^d_i & j\le d,\\ \beta^d_i & j>d,\end{cases}$$

but there is no overlap in the blending functions of the centre column of control points. For a degree d patch the extraordinary faces should be separated by at least $d-1$ layers of regular faces. This time the local parameters s_i and h_i need to be scaled by d to encompass the extended intervals, resulting in the patch definition

$$\mathbf{S}^d(\phi)=\sum_{i=0}^{n}\mathbf{R}_i(ds_i,dh_i).$$

4.3. Continuity

The d-degree multisided B-spline patches are G^{d-1} continuous with respect to neighbouring regular regions and other multisided B-spline patches. This can easily be seen from the construction of the B-spline ribbons and their associated blending functions. We want to show that the only ribbon that contributes positionally and differentially towards the patch on the boundary Γ_i is $\mathbf{R}_i$. Let us examine a control point towards the left side of ribbon $\mathbf{R}_i$, which is shared with $\mathbf{R}_{i-1}$, and its associated basis function:

$$\alpha^d_i B(s_i,h_i)+\beta^d_{i-1}C(s_{i-1},h_{i-1}), \tag{2}$$

where

$$\begin{aligned}B(u,v) &= N^d_j(u)E^d_k(v) \quad \text{of} \quad \mathbf{R}_i \quad \text{and}\\ C(u,v) &= N^d_{d-k}(u-1)E^d_j(v) \quad \text{of} \quad \mathbf{R}_{i-1}.\end{aligned}$$

The blending functions α^d_i and β^d_i have the following properties on Γ_i

$$\begin{aligned}&\alpha^d_i\Big|_{\Gamma_i}=1, \quad \partial^j\alpha^d_i\Big|_{\Gamma_i}=0, \quad \forall j>0,\\ &\beta^d_{i-1}\Big|_{\Gamma_i}=0, \quad \partial^j\beta^d_{i-1}\Big|_{\Gamma_i}=0, \quad \forall j>0,\end{aligned}$$

where the derivative is taken in some direction not parallel to s_i. By taking the p-th derivative ∂^p of (2) in a particular direction not parallel to s_i on Γ_i, we thus obtain

$$\begin{aligned}&\partial^p(\alpha^d_i)B(s_i,0)+\alpha^d_i\partial^p(B(s_i,h_i))|_{h_i=0}+\partial^j(\beta^d_{i-1})C(1,h_{i-1})+\\ &\beta^d_{i-1}\partial^j(C(s_{i-1},h_{i-1}))|_{s_{i-1}=1}\\ =&0\cdot B(s_i,0)+1\cdot\partial^p(B(s_i,h_i))|_{h_i=0}+0\cdot C(1,h_{i-1})+\\ &0\cdot\partial^j(C(s_{i-1},h_{i-1}))|_{s_{i-1}=1}\\ =&\partial^p(B(s_i,h_i))|_{h_i=0}.\end{aligned}$$

This is exactly the p-th derivative of the basis functions of the ribbon $\mathbf{R}_i$, which is what we set out to show. This shows that only the ribbon associated with Γ_i contributes to this side, and that the multisided patches will reproduce the derivatives of their input B-spline ribbons. This process also happens analogously with respect to $\mathbf{R}_{i+1}$, and therefore the patches connect with G^{d-1} continuity. Internally the patches are C^{d-1} because the B-spline ribbons they are constructed from are C^{d-1} continuous.

5. Results

In this section we examine the visual quality of the proposed multisided constructions. We also provide and test several adjusted basis functions that improve the shape of the patches.

5.1. Effect of Normalisation

In Figure 5 we highlight the effect normalisation has on the patches. Especially in the quadratic case it becomes apparent that the normalisation flattens the patches off towards the centre of the surfaces. This effect becomes less prominent when considering higher degree patches, but is still apparent in high valency patches. For extraordinary face patches this effect is even more noticeable; see the bottom row of Figure 5. For these EF patches the flatness becomes even more apparent, because of the reduced sum of the basis functions. This can be clearly seen when examining the weight deficiency of the patches.

In Figure 6 we show the sum of the weights $f(\phi)$ (see (1)) for patches of various valencies and degrees. As can be seen, the deficient weight increases with valency and with degree for both EV

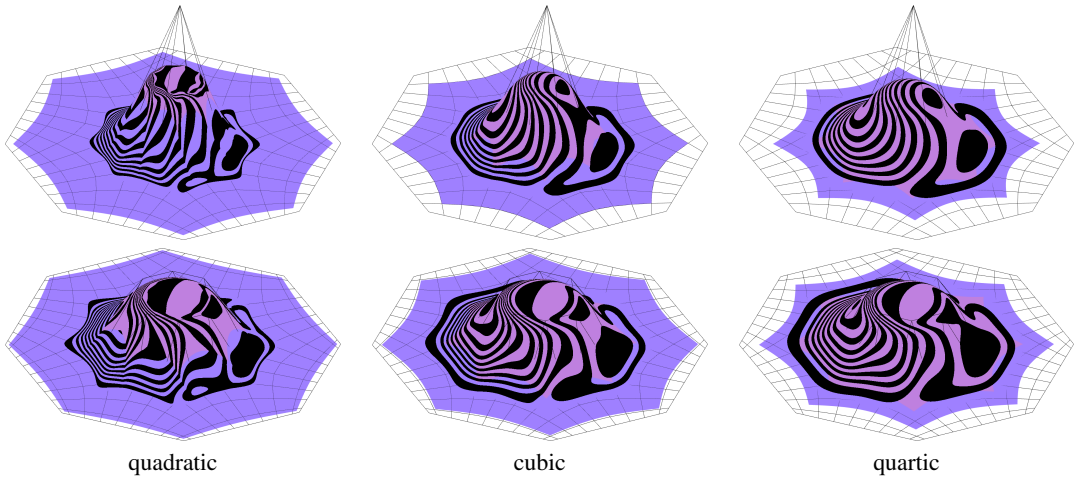

Figure 5: Reflection lines visualisations at an octagonal extraordinary vertex (top row) and face patches (bottom row) for different degrees of multisided B-spline patches.

and EF patches. This shows that the (deficient) weight is a major factor that influences the shape of the resulting patches. Motivated by this observation, we design special basis functions that improve the shape of the patches in the next section.

5.2. Central Control Point Functions

Instead of using an additional control point to attach the deficient weight to, as with the cubic multisided patch (Section 3.2), we can design different expressions for the basis functions of the central control point for EV patches, or the central ring of control points of EF patches. When doing this we have to make sure that these functions, like the extended basis functions, vanish on distant sides of the patches and connect smoothly with the basis functions of adjacent regions. In this manner we can tune the influence of different control points towards the centre of the patches while maintaining the smooth connection with adjacent patches. We attach the relevant functions to certain control points of the patch, but we only use them for the h_i parameter of each ribbon, thereby changing the shape of the ribbon surfaces in the parametric directions going into the patch.

We start with the quadratic patches, as the effect of normalisation is the most pronounced there. We have designed a function that depends on a parameter, ρ, which controls the weight of the patch; it can lead even to an excess of weight. The centre function for a quadratic EV patch is a C^1 piece-wise cubic function on $[0,1]$ (see Figure 9), defined as

$$V_1^2(u) = \begin{cases} \frac{1}{2}(1-2u)^3 + 4(1-2u)^2 u & u \in [0, \frac{1}{2}], \\ +3\rho(1-2u)(2u)^2 + \rho(2u)^3 & \\ \rho(2-2u)^3 + 3\rho(2-2u)(2u-1) & u \in [\frac{1}{2}, 1]. \end{cases}$$

By adjusting ρ, we can increase the weight of the patches towards the centre, as shown in Figure 7. Observe how the combination of basis functions attached to the centre control point has improved the fullness of the quadratic EV patches. The process can also be applied to for quadratic EF patches by choosing slightly different functions, and even for cubic EV and EF patches. In Appendix A we detail several adjusted functions for the central control points that we created. In Figure 8, we show the difference between using the standard extended basis functions or using our handpicked ones for quadratic EF patches. And Figure 10 shows the difference between the standard extended cubic basis functions and our adjusted ones. In all cases the flatness towards the centre is alleviated and improved fullness is achieved.

Naturally, the same process can be done for higher-degree patches as well. However, as their extended basis functions consist out of more individual polynomial pieces, the functions have a more complicated definition, due to a higher number of derivatives that have to be matched. Furthermore, the shape of the functions must be considered carefully, as oscillating or otherwise poorly shaped functions will also show clear changes in the resulting patches.

6. Discussion & Conclusion

Even though the weight deficiency remains an issue, the adjustment of the basis functions attached to the centrally placed control points is able to resolve the flatness towards the centre of the patches in case of extraordinary vertex and extraordinary face patches. Another choice we considered was to degree-elevate the patches and in turn create extra control points that can influence the shape. However, this takes away from the simplicity of the patches, which we believe should not stray too far from the generalisation of tensor-product B-spline patches to the multisided setting. As a result, our construction derives all the needed information for the patches from the control mesh itself, without requiring the user to specify or adjust any further control points or parameters.

The input meshes require a separation of extraordinary regions, especially when the degree of the patches is increased. This may limit the usability of the method as for general meshes a few initial steps of subdivision are required or special care must be taken

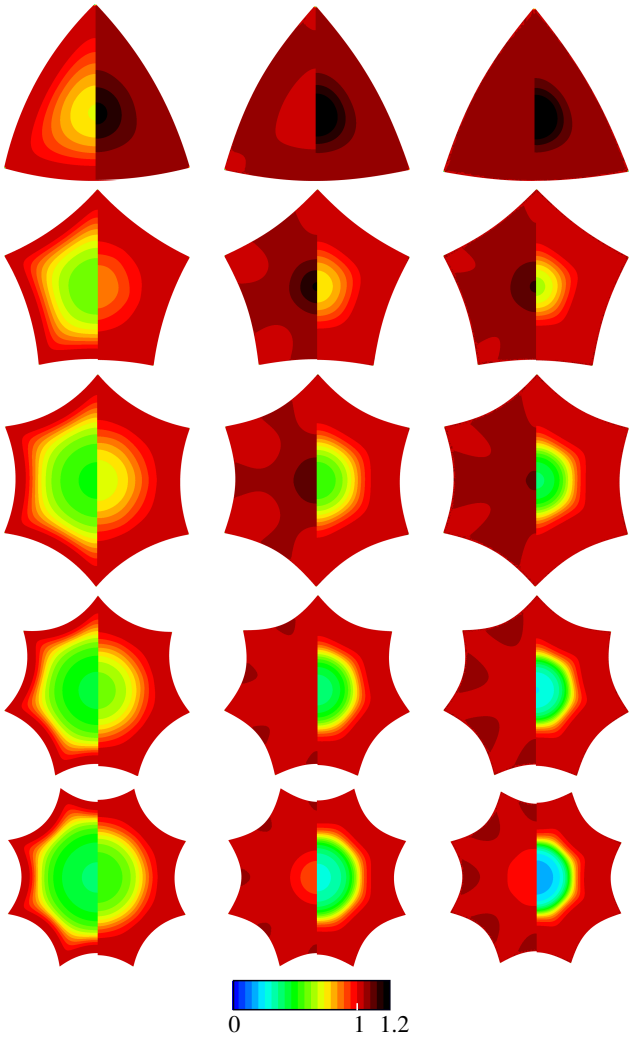

Figure 6: *Weight deficiency/excess for triangles, and pentagons up to octagons. Left to right column: the quadratic, cubic and quartic case. Each image shows the sum of weights for EV patches on the left and EF patches on the right.*

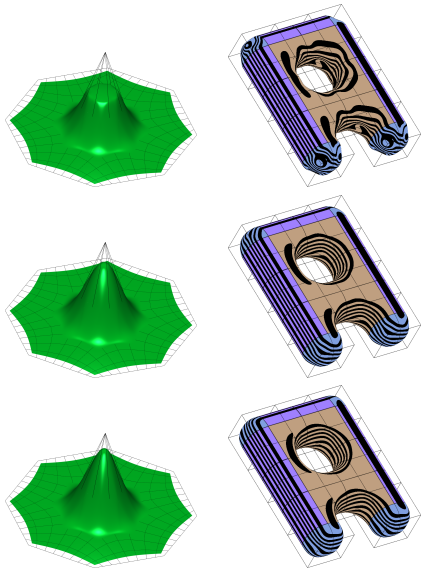

Figure 7: Left column: A quadratic octagonal EV patch. Right column: An object with several valency 3 and 5 quadratic EV patches. From top to bottom: Standard extended basis functions, with centre functions with $\rho = \frac{3}{4}$, and with $\rho = 1$.

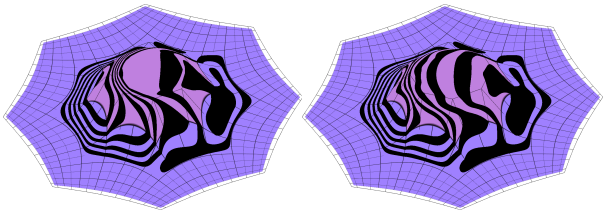

Figure 8: Reflection line renderings of a quadratic EF patch. Left: with standard extended basis functions. Right: using $F_0^2(u)$ and $F_1^2(u)$.

whilst designing the meshes. Even though the number of control points grows with the degree of the patches it is still feasible to render the patches in real-time using hardware tessellation. We have implemented patches up to degree 4 for patches with a maximum of 8 sides for both the extraordinary vertex and face techniques. Using the same approach taken in [HBK18] we are able to achieve interactive rates of performance using hardware tessellation.

We have presented a generalisation of the multisided B-spline construction for B-spline surfaces of arbitrary bi-degree. We have also shown that the previous construction can be adjusted to span surfaces over extraordinary faces, by extending the number of intervals used in the B-spline ribbons. The patches join with G^{d-1} continuity to adjacent patches and internally are C^{d-1} smooth. For arbitrary topology meshes they can be used in combination with a few steps of arbitrary degree subdivision methods. The patch structure remains simple and can easily be rendered using modern graphics hardware. We have also shown how to create different basis functions for certain control points in the patches so as to improve the overall shapes. As the majority of multisided patch constructions suffers from decreased shape quality for higher valencies, this remains a challenging direction for future research.

Acknowledgements
We gratefully acknowledge the support of NVIDIA Corporation with the donation of the Titan V GPU used for this research.

Appendix A: Central Control Point Functions

To improve the visual appeal of the patches we have determined some (tunable) expressions for the basis functions that are attached to certain control points of the ribbons.

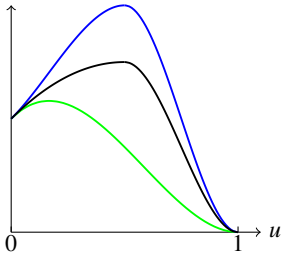

Figure 9: The proposed cubic function $V_1^2(u)$ attached to the central control point in quadratic EV patches. The original $N_1^2(u)$ is shown in green, the adjusted function with $\rho = \frac{3}{4}$ in black, and the adjusted function with $\rho = 1$ in blue.

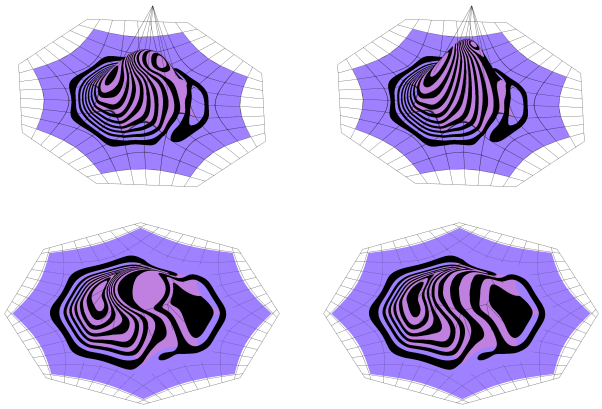

Figure 10: Reflection line renderings of, top row: octagonal extraordinary vertex patch, bottom row: octagonal extraordinary face patch. Left column: without adjusted centre basis functions and, right column, with adjusted centre basis functions.

We first define

$$B[a_0, a_1, \ldots, a_d](u) = \sum_{i=0}^{d} a_i B_i^d(u)$$

with $B_i^d(u)$ the Bernstein polynomials of degree d. In other words, the sequence $[a_0, a_1, \ldots, a_d]$ are the control values of the polynomial in the Bernstein-Bézier form.

All of the below-constructed functions satisfy the needed value and derivative constraints at the start and end of their intervals of definition, and they are built in such way that they are always at least C^1 for quadratic patches and C^2 for cubic patches.

We create the following basis functions for quadratic EF patches:

$$F_0^2(u) = \begin{cases} B[\frac{1}{2}, \frac{5}{6}, b, a](u) & u \in [0,1], \\ B[a, 2a-b, 0, 0](u-1) & u \in [1,2], \end{cases}$$

and

$$F_1^2(u) = \begin{cases} B[\frac{1}{2}, \frac{1}{2}, \bar{b}, \bar{a}](u) & u \in [0,1], \\ B[\bar{a}, 2\bar{a}-\bar{b}, 0, 0](u-1) & u \in [1,2]. \end{cases}$$

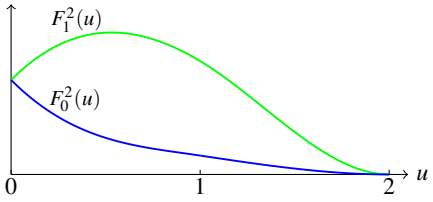

Figure 11: Adjusted extended basis functions for the centrally placed control points of quadratic EF patches: $F_0^2(u)$ (blue) and $F_1^2(u)$ (green).

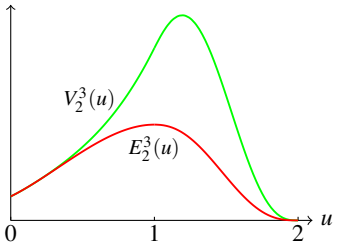

Figure 12: Adjusted extended basis function for the central control point of cubic EV patches. $V_2^3(u)$ (green) and $E_2^3(u)$ (red).

We chose the parameters $a = 0.6, b = 0.8$ and $\bar{a} = 0.1, \bar{b} = 0.23$. No matter what values are chosen for a and b, the functions are always C^1. The functions are this time attached to not only the centrally placed control points, but rather all extended basis functions in the h_i direction are replaced by these new expressions. The functions are shown in Figure 11.

We created the following expression for the adjusted extended basis function as a piece-wise quintic Bézier function with coefficients for cubic EV and EF patches respectively:

$$V_2^3(u) = \begin{cases} B^5[\frac{1}{6}, \frac{4}{15}, \frac{5}{12}, \frac{55}{100}, \frac{4}{5}, \frac{6}{5}](u) & u \in [0,1], \\ B^5[\frac{6}{5}, \frac{12}{5} - \frac{4}{5}, \frac{12}{5} - \frac{55}{100}, 0, 0, 0](u-1) & u \in [1,2], \end{cases}$$

and

$$F_2^3(u) = \begin{cases} D_2^3(u) & u \in [0,1], \\ B^5[\frac{2}{3}, \frac{2}{3}, \frac{17}{30}, \frac{2}{5}, \frac{2}{5}, \frac{2}{5}](u-1) & u \in [1,2], \\ B^5[\frac{2}{5}, \frac{2}{5}, \frac{2}{5}, 0, 0, 0](u-2) & u \in [2,3]. \end{cases}$$

The functions are shown and compared to the normal extended basis functions in Figures 12 and 13, respectively.

References

[Flo15] FLOATER M. S.: Generalized barycentric coordinates and applications. *Acta Numerica 24* (2015), 161–214.

[GLZ90] GREGORY J. A., LAU V. K., ZHOU J.: Smooth parametric surfaces and n-sided patches. In *Computation of curves and Surfaces*. Springer, 1990, pp. 457–498.

[HBK18] HETTINGA G. J., BARENDRECHT P. J., KOSINKA J.: A comparison of GPU tessellation strategies for multisided patches. In *EG 2018 - Short Papers* (2018), The Eurographics Association, pp. 45–48.

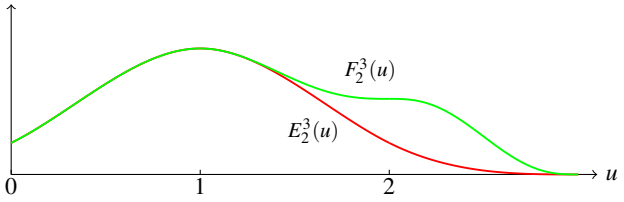

Figure 13: Adjusted extended basis function for the ring of central control points of cubic EF patches. $F_2^3(u)$ (green) and $E_2^3(u)$ (red).

[HK20] HETTINGA G. J., KOSINKA J.: A multisided C^2 B-spline patch over extraordinary vertices in quadrilateral meshes. *Computer-Aided Design 127* (2020), 102855.

[KP16] KARČIAUSKAS K., PETERS J.: Minimal bi-6 G^2 completion of bicubic spline surfaces. *Computer Aided Geometric Design 41* (2016), 10–22.

[LD89] LOOP C. T., DEROSE T. D.: A multisided generalization of Bézier surfaces. *ACM Transactions on Graphics (TOG) 8*, 3 (1989), 204–234.

[LS08] LOOP C., SCHAEFER S.: G^2 tensor product splines over extraordinary vertices. In *Computer Graphics Forum* (2008), vol. 27, Wiley Online Library, pp. 1373–1382.

[LSNC09] LOOP C., SCHAEFER S., NI T., CASTAÑO I.: Approximating subdivision surfaces with Gregory patches for hardware tessellation. In *ACM Transactions on Graphics (TOG)* (2009), vol. 28, ACM, pp. 151:1–151:9.

[NG00] NAVAU J. C., GARCIA N. P.: Modeling surfaces from meshes of arbitrary topology. *Computer Aided Geometric Design 17*, 7 (2000), 643–671.

[Pet02] PETERS J.: C^2 free-form surfaces of degree (3,5). *Computer Aided Geometric Design 19*, 2 (2002), 113–126.

[Pet19] PETERS J.: Splines for meshes with irregularities. *The SMAI journal of computational mathematics S5* (2019), 161–183.

[Sta98] STAM J.: Exact evaluation of Catmull-Clark subdivision surfaces at arbitrary parameter values. In *Proceedings of the 25th annual conference on Computer graphics and interactive techniques* (1998), pp. 395–404.

[Sta01] STAM J.: On subdivision schemes generalizing uniform B-spline surfaces of arbitrary degree. *Computer Aided Geometric Design 18*, 5 (2001), 383–396.

[SV18] SALVI P., VÁRADY T.: Multi-sided Bézier surfaces over concave polygonal domains. *Computers & Graphics 74* (2018), 56–65.

[VSK16] VÁRADY T., SALVI P., KARIKÓ G.: A multi-sided Bézier patch with a simple control structure. In *Computer Graphics Forum* (2016), vol. 35, Wiley Online Library, pp. 307–317.

[VSVS20] VÁRADY T., SALVI P., VAITKUS M., SIPOS Á.: Multi-sided bézier surfaces over curved, multi-connected domains. *Computer Aided Geometric Design 78* (2020), 101828.

[Wac75] WACHSPRESS E.: *A Rational Finite Element Basis*. Academic Press, 1975.

[YZ04] YING L., ZORIN D.: A simple manifold-based construction of surfaces of arbitrary smoothness. *ACM Trans. Graph. 23*, 3 (Aug. 2004), 271–275.

[ZZZS05] ZHENG J. J., ZHANG J. J., ZHOU H. J., SHEN L. G.: C^2 continuous spline surfaces over Catmull-Clark meshes. In *Computational Science and Its Applications – ICCSA 2005* (2005), Springer Berlin Heidelberg, pp. 1003–1012.